Final Report:
Grant Number: NCC5-707
Investigation Group: CD-01

Title: Spatial integration of Regional Carbon Balance in Amazonia

PIs: Allan Scott Denning - Colorado State University
Pedro Leite da Silva Dias - IAG/USP

1. Narrative of activities

1.1 Summary of Activities

We have completed a three-year investigation of land-atmospheric CO_2 exchange over Amazon Basin. During the project time span, we have implemented and evaluated a new version of ecophysiology model SiB that is capable of realistically representing seasonal drought in surface fluxes of carbon, energy, and water. Significant modifications have been made to the calculation of soil water stress on photosysthesis, and with the radiative transfer module. The improved SiB3 parameterizations are able to reproduce the observed inter-annual variations and seasonality in net ecosystem exchange, sensible, and latent heat fluxes reasonably well. The linkage of SiB model with Regional Atmospheric Modeling System (RAMS) has been completed, and the coupled modeling system has been applied to Tapajos region to simulate mesoscale circulations and atmospheric CO_2 variations during the dry season 2001 Santarem field campaign. The model is able to capture the observed meteorology and CO_2, as well as surface fluxes of CO_2, H, and LE, for the 15-day simulation time period. The mechanically forced low-level convergence proves to have significant impact on observed ecosystem carbon fluxes, and should be taken into account if tower fluxes are to be generalized to a large region. The impact of CO_2 evasion from the Tapajos River has also been evaluated by performing numerical sensitivity experiments with and without river CO_2 effluxes. The results show that the river CO_2 effluxes increase carbon uptake over vegetated land due to short-term CO_2 fertilization effects. The Amazon Basin stays a carbon sink despite of the river CO_2 evasion. However, to study the long-term effects of atmospheric CO_2 enrichment, a more sophisticated ecosystem model that can account for nitrogen limitation may lead to a different conclusion. As part of the BARCA field experiment, we compared aircraft and flux tower sampling strategies using SiBRAMS and LPDM trajectory model, and recommend that continuous tower based high precision [CO_2] measurements can reduce uncertainty in global atmospheric inversions and therefore in our understanding of the global carbon budget. Finally, our fine-resolution SiBRAMS Amazon simulations, combined with emulated satellite tracks, are utilized to estimate spatial and temporal representation errors in inversions of orbiting carbon observatory (OCO) CO_2 retrievals.

1.2 Parameterizing the ecophysiology of seasonal drought -- SiB3 model development

Realistically representing ecophysiology of seasonal drought has been a focus for our LBA project. New developments in the SiB code (Baker et al, in preparation) have positive ramifications for simulations of the LBA ecoregion. We have made significant modifications to the calculation of soil water stress on photosynthesis, as well with the radiative transfer submodel. These alterations improve biophysical realism in SiB, and improve simulated quantities output from the model.

a. Soil Water Stress

Traditionally, biophysical models have had difficulty reproducing the annual cycle of Net Ecosystem Exchange of Carbon (NEE) (Figure 1) in Amazon regions. NEE is essentially the sum of respiratory efflux-a function of moisture and temperature-and photosynthetic uptake by plants.

Observational data shows that the magnitude of the photosynthetic flux does not have a large annual cycle; recent evidence (Saleska et al, 2005) that there may in fact be a slight increase in photosynthesis during the dry season, presumably in response to increased radiative forcing. Observed annual NEE cycle appears to be driven by a decrease in respiration during the dry season as bacterial activity in near-surface soil layers subsides in response to drying. The net result is biospheric uptake of carbon during the dry season, and efflux during the wet season.

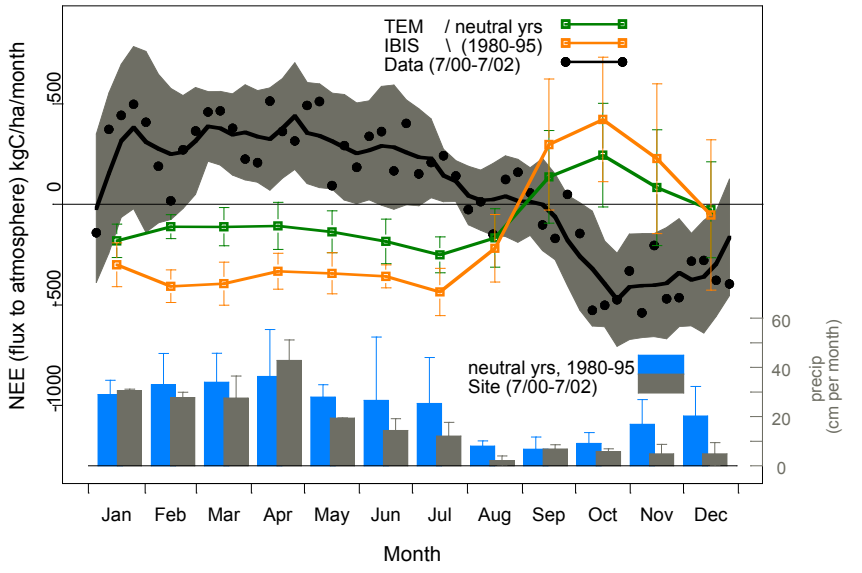

Figure 1: Mean seasonal NEE and precipitation (± SD of interannual variation) in the Tapajós National Forest, Brazil. Model Output from: TEM (Tian et al, 1998, 2000) & IBIS (Botta & Foley, 2002) models (8 years, colored lines) Data from Tapajos Forest eddy flux sites (black line is moving average monthly NEE ± SD, points are average weekly NEE)

Most biospheric models, SiB included, have responded to drying conditions by decreasing photosynthetic flux. In some cases, modeled uptake of carbon is reduced to almost dormant levels during the dry season. Additionally, respiratory flux has can increase in response to rising soil temperatures. The net effect of seasonal changes in respiration is an increase during the dry season-respiration increase due to rising temperature exceeds respiratory decrease due to drying soils. The net effect is modeled NEE that is 180 degrees out of phase with observations; influx during the wet season, efflux during dry.

It has been observed that Amazon vegetation responds to lack of moisture in near-surface soil layers by tapping water deep in the soil that maintains water levels through periods of drought. Root mass/density is not large in these deep layers, but physiological response is such that the vegetation can maintain normal levels of photosynthetic activity by altering the region of the soil where water is drawn (Jipp et al, 1998). By altering where to 'look' for water, the vegetation function is maintained as water in the soil rises and falls.

To date, biophysical models have been unable to reproduce this aspect of vegetation function; modeled transpirational load has been determined by root density alone, which generally follows an exponential decrease with depth following published maps (Jackson et al, 1996). Models have not been able to tap into deep water to fill transpirational load. We seek to reproduce observed biophysical function by combining model root density profile with an 'apparent' root density that is a function of water content. In this way, the vegetation in SiB can draw on deep soil water during periods when surface layers are dry. During wet periods, transpiration burden will be borne by near-surface layers where root density is highest. This is a modified 'bucket' approach, where root density determines the initial profile of water drawn from the soil, yet water from the entire soil column can be tapped during periods of stress.

Model formulation achieves this function by considering both whole-column and layer-specific processes. Initially, stress is calculated by determining the column-mean volumetric water content and moisture potential. Canopy-scale soilwater stress is determined to be zero when colum-mean potential is greater than field capacity, defined to be where $\mu \geq -15$ J/kg (Cassel and Nielsen, 1986). When potential is below wilting point (defined as $\mu < -1500$ J/kg), soil water stress is considered total, and no transpiration will occur. At intermediate column-mean levels of water content, water stress is calculated as follows:

$$STRESS = \frac{\left(\left[1 + w_{stress} \right] \theta_{column} \Big/ \theta_{field\_capacity} \right)}{\left(w_{stress} + \theta_{column} \Big/ \theta_{field\_capacity} \right)}$$

where a stress value of 1 indicates unstressed photosynthesis and 0 results in total photosynthetic shutdown. Once a canopy-scale stress level has been determined, the transpirational load is distributed between individual soil layers by determining an 'apparent' root density for each layer, R^*_i as a function of initial root density F and water content θ:

$$R_i^* = F_i \left(\frac{\left[1 - \theta_{wilt} / \theta_i \right]}{\left[1 - \theta_{wilt} / \theta_{field\_capacity} \right]} \right)$$

The 'apparent' root fractions, R^*_i, are then normalized to get individual layer contributions:

$$R_i^* = \frac{R_i^*}{\sum_{i=1}^{nsoil} R_i^*}$$

This allows for a given soil layer to contribute to total transpiration at a level above that which specified root fraction would allow.

Another recent model development is the installation of a canopy radiative scheme that explicity treats sunlit and shaded portions of the canopy. SiB has had a tendency, in dense canopies that do not experience severe water stress (see Baker et al, 2003) to simulate a Bowen Ratio (ratio of sensible to latent heat) much larger than observed.

b. Radiative Transfer

SiB History: Continuous Canopy

Radiative transfer in SiB follows Sellers (1985), which calculates canopy energy budget on the basis of total beam, diffuse and scattered (transmitted and reflected) light as the solution to equations from Dickinson (1983) given in the appendix of Sellers (1985). The transfer of light through the canopy takes the following form:

$$-\bar{\mu}\left(dI\uparrow / dL\right) + \left[1-(1-\beta)\omega\right] I\uparrow - \omega\beta I\downarrow = \omega\bar{\mu}K\beta_0 \exp(-KL)$$
$$\bar{\mu}\left(dI\downarrow / dL\right) + \left[1-(1-\beta)\omega\right] I\downarrow - \omega\beta I\uparrow = \omega\bar{\mu}K\left(1-\beta_0\right)\exp(-KL)$$

Total canopy conductance and assimilation of carbon is treated separately; stomatal resistance is calculated for a square meter of sun-leaf, and canopy-scale conductance and associated model diagnostics are determined on the basis of satellite-derived parameters, particularly fPAR (fraction of absorbed Photosynthetically Active Radiation) which is calculated from Normalized-Difference Vegetation Index (NDVI). The calculation is similar to a Beers-Law type of exponential extinction law, where

$$\int_0^{L_T} e^{-KL} dL = \frac{\left(1 - e^{K L_T}\right)}{K} = \frac{fPAR}{K} = \Pi$$

and the coefficient Π is multiplied with sun-leaf photosynthesis to scale from leaf-level to the full canopy. In this regard, SiB is not a big-leaf model; it is an infinite-leaf model, and

uses the continuous distribution of nitrogen through the canopy and its analog to direct-beam light extinction to scale photosynthesis from leaf- to canopy-scale.

While this expression of radiative transfer represents an improvement from traditional big-leaf models, we've been experimenting with a further refinement of the code, in which sunlit and shaded fractions of the canopy are treated explicitly. The new treatment is more biophysically representative, and has the further benefit that radiative transfer of light for both photosynthesis and canopy heating are treated in an internally consistent manner.

Sunlit/Shaded Radiative Submodel

For the SUnlit/SHaded Integration (SUSHI) formulation, we use the albedo determined previously in the Continuous Canopy method, which follows Sellers (1985). These albedos are determined by the solution to equations (1) and (2) from Sellers 1985 as given in Appendix A of that paper.

$$-\bar{\mu}\left(dI\uparrow/dL\right)+\left[1-(1-\beta)\omega\right]I\uparrow-\omega\beta I\downarrow=\omega\bar{\mu}K\beta_0\exp(-KL)$$

$$\bar{\mu}\left(dI\downarrow/dL\right)+\left[1-(1-\beta)\omega\right]I\downarrow-\omega\beta I\uparrow=\omega\bar{\mu}K\left(1-\beta_0\right)\exp(-KL)$$

From Sellers (1985): "$I\uparrow$ and $I\downarrow$ are the upward and downward diffuse radiative fluxes, normalized by the incident flux, μ is the cosine of the zenith angle of the incident beam, K is the optical depth of direct beam per unit leaf area and is equal to G(μ)/μ, G(μ) is the relative projected area of leaf elements in the direction cos-1μ, $\bar{\mu}$ is the average inverse diffuse optical depth per unit leaf area and is equal to $\int_0^1\left[\mu'/G\left(\mu'\right)\right]d\mu'$, μ' is the direction of scattered flux, ω is the scattering coefficient and is equal to $\alpha+\tau$, α is the leaf-element reflectance, τ is the leaf-element transmittance, and L is the cumulative leaf-area index."

Next, we calculate the absorption factors for sunlit and shaded canopy fractions from equations given in de Pury and Farquhar (1997); ground absorption factors are unchanged from those given in Sellers (1985). Radiation absorbed by sunlit leaves is given in de Pury and Farquhar's equations 20(a-d), while radiation absorbed by shaded leaves is given by equations A26(a-c). Radiation absorbed by the sunlit fraction of the canopy is the sum of beam, diffuse and scattered-beam components as follows:

$$I_{sunlit}=\int_0^{L_T}I_{beam}(L)f_{sunlit}(L)dL+\int_0^{L_T}I_{diffuse}(L)f_{sunlit}(L)dL$$

$$+\int_0^{L_T}I_{scattered\_beam}(L)f_{sunlit}(L)dL$$

The solution to the first part of the equation, beam radiation absorbed sunlit leaves, is

$$\int_0^{L_T} I_{beam} f_{sunlit}(L)dL = I_{beam}(0)(1-\sigma)\left[1-\exp\left(-k_b L_T\right)\right]$$

where $I_{beam}(0)$ is the direct-beam radiation at the top of the canopy, σ is the scattering coefficient (given as 0.15 in de Pury and Farquhar always; we use $\sigma = \tau + \alpha$ which is analogous to the term ω from Sellers (1985); hereafter, we will replace σ with ω in the radiative transfer equations), L_T is total Leaf Area Index (LAI) and kb is the direct beam extinction coefficient of the canopy $\left(k_b = 0.5/\sin\beta\right)$ where β is the solar elevation angle (the complement of zenith angle, ω). Diffuse radiation absorbed by sunlit leaves is given by

$$\int_0^{L_T} I_{diffuse}(L) f_{sunlit}(L)dL = I_{diffuse}(0)\left(1-\rho_{cd}\right)\frac{\left\{1-\exp\left[-\left(k_d^{'}+k_b\right)L_T\right]\right\}k_d^{'}}{\left(k_d^{'}+k_b\right)}$$

and direct-beam radiation that is scattered and absorbed by sunlit leaves is given by

$$\int_0^{L_T} I_{scattered\_beam}(L) f_{sunlit}(L)dL = I_{beam}(0)\left(1-\rho_{beam}\right)\frac{\left\{1-\exp\left[-\left(k_b^{'}+k_b\right)L_T\right]\right\}k_b^{'}}{\left(k_b^{'}+k_b\right)}$$

$$-(1-\omega)\frac{\left[1-\exp\left(-2k_b L_T\right)\right]}{2}$$

For shaded fraction of the canopy, the fraction of leaf that is not illuminated by direct sunlight is given by $f_{shaded} = 1 - f_{sunlit}$, and absorbed radiation is given by $I_{shaded} = I_{total} - I_{sunlit}$. There is no direct-beam component for shaded leaves, so that total illumination of shaded leaves is a function of diffuse and scattered-beam radiation only, as follows:

$$I_{shaded} = \int_0^{L_T} I_{diffuse}(L)\left[1-f_{sunlit}(L)\right]dL + \int_0^{L_T} I_{scattered\_beam}(L)\left[1-f_{sunlit}(L)\right]dL$$

The two components of shaded-leaf absorbed radiation-diffuse and scattered beam-are represented by

$$\int_0^{L_T} I_{diffuse}(L)\left[1-f_{sunlit}(L)\right]dL = I_{diffuse}(0)\left(1-\rho_{diffuse}\right)\times$$

$$\left[1-\exp\left(k_d^{'}L_T\right)-\frac{\left\{1-\exp\left[-\left(k_d^{'}+k_b\right)L_T\right]\right\}k_d^{'}}{\left(k_d^{'}+k_b\right)}\right]$$

and

$$\int_0^{L_T} I_{scattered\_beam}(L)\left[1-f_{sunlit}(L)\right]dL = I_{beam}(0)\times$$

$$\left[\begin{array}{l}\left(1-\rho_{beam}\right)\left(1-\exp\left(-k_b' L_T\right)-\dfrac{\left\{-\exp\left[-\left(k_b'+k_b\right)L_T\right]\right\}k_b'}{\left(k_b'+k_b\right)}\right)\\ -(1-\omega)\dfrac{\left\{1-\exp\left(-k_b L_T\right)-\left[1-\exp\left(-2k_b L_T\right)\right]\right\}}{2}\end{array}\right]$$

respectively.

Canopy Radiation: Results and Discussion;

NEE calculated using the SiB Continuous Canopy formulation for Tapajos River km83 site and plotted against incoming net radiation is shown in Figure 2. These data represent years 2002-2004 and encompass both wet and dry seasons. SiB Continuous Canopy (CC) NEE saturates at around –20 μmol m^{-2} sec^{-1} at a radiation value near 150 W and is constant at higher irradiance levels. When compared to observed NEE vs. radiation, it can be seen that SiB-CC at low light levels, and the amplitude of the maximum influx (and efflux) is too low. We propose that early saturation occurs because canopy-scale photosynthesis is represented by the behavior of a single leaf. Leaf-level measurements have indicated that leaf response is discrete between light-limited and enzyme-limited regimes (Sellers et al 1992), and SiB response has been constructed to reproduce this behavior. However, canopy-scale behavior can be expected to differ from an individual leaf as the vegetation allocates photosynthetic material and alters leaf-angle distribution for maximum utilization of available light (Wang and Jarvis 1993, Meir et al 2002) in such a way that the canopy-scale response is more linear, such as in Figure 3.

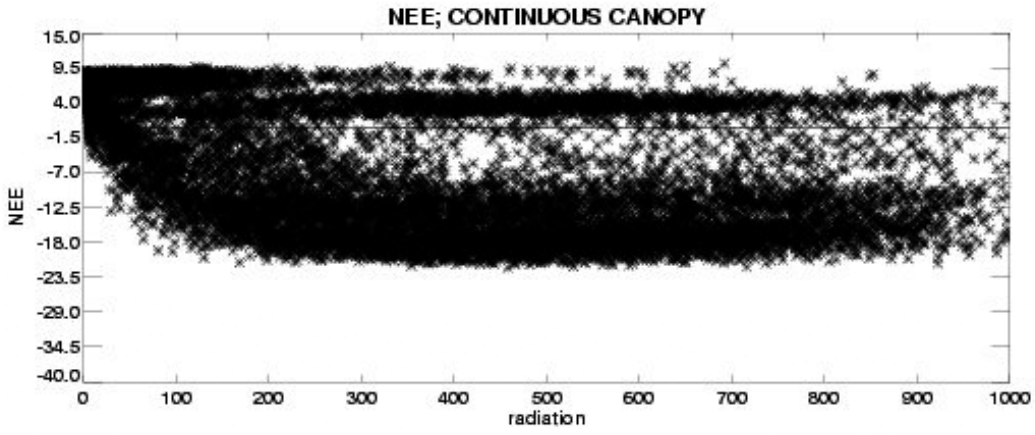

Figure 2: Net Ecosystem Exchange of Carbon (NEE) at Tapajos River km83 Tower. NEE is calculated using SiB with the Continuous Canopy radiative submodel plotted vs. radiation in Watts for years 2002-2004. Flux into the canopy is negative.

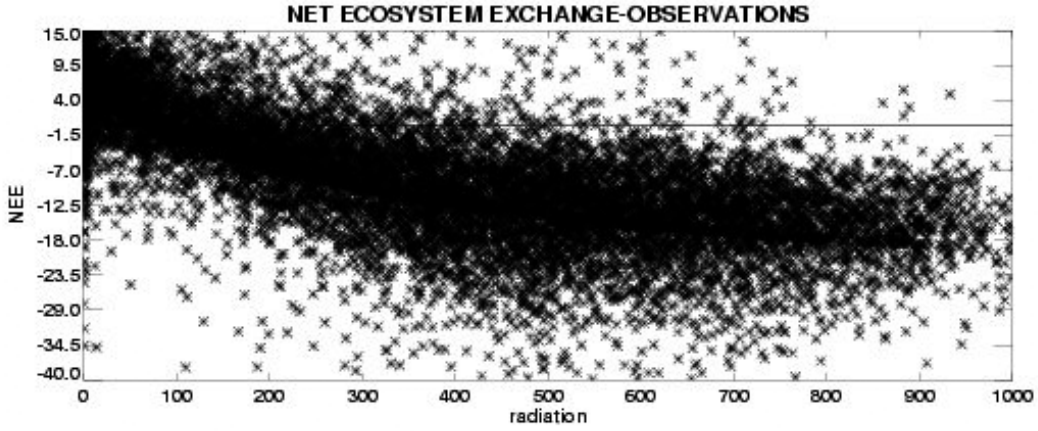

Figure 3: Observed NEE at Tapajos River km83 Tower, plotted vs. radiation in Watts, for years 2002-2004.

Furthermore, it is obvious that modeled NEE using SiB-CC does not reproduce maximum influx at high light levels; the model reaches a cap, or maximum NEE influx at low light levels and does not have the ability to accommodate high light. This is shown in Figure 4, which shows modeled vs. observed NEE. Model values-both influx and efflux-are capped at low-magnitude values when compared to observations. We believe that the combination of dense canopy and low water limitation result in a situation at high light levels where the model does not allow sufficient photosynthesis (and attendant transpiration) to adequately cool the canopy. In this case, photosynthesis does not increase with increasing light levels, resulting in poor comparison to observed NEE as well as increased Bowen Ratio when compared to obs. It should be noted that as annual respiration is tied to photosynthesis by the annual-mean zero-sum assumption in SiB NEE (Denning et al, 1996), that respiratory flux will be constrained in a manner similar to influx.

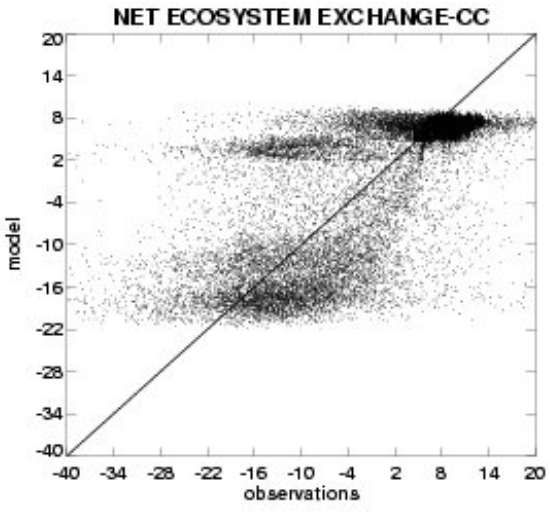

Figure 4: Observed (X-axis) vs. Modeled (Y-axis) NEE for the Tapajos River km83 Tower. Model used is SiB with Continuous Canopy radiative scheme.

By incorporating the Sunlit/Shaded canopy radiative scheme (SUSHI), we hope to more closely reproduce the observed behavior of canopy-level NEE with increasing light, as well as increase the magnitude of maximum influx/efflux situations. As the SUSHI radiative submodel is self-consistent in its treatment of canopy heating and photosynthetic forcing, the Modeled Bowen Ratio should be closer to the observed. Canopy acclimation is captured by the explicit treatment of sunlit and shaded leaves, so the linearity of the NEE vs. light response should be more accurately represented as well. This is seen in Figure 5, which shows NEE vs. radiation for the SiB-SUSHI scheme. Maximum influx and efflux have larger values when compared to SiB-CC, and the response at low light levels is more linear in the SUSHI simulation than in CC.

Finally, the modeled (SiB-SUSHI) vs. NEE for this site is shown in Figure 6. The slope of the points at intermediate values is still >1, which implies that the model still responds too quickly to changing conditions at intermediate levels within the climatic range. Maxima are not exactly captured either. However, the overall response is much better. The modeled NEE values are much closer to a slope of 1. The modeled Bowen Ratio is also much improved, as shown in Figure 7. SiB-CC simulations have elevated BR during daylight hours, while SiB-SUSHI simulations are quite close to observed. This will have a significant impact on carbon flux as well as on the meteorology simulated in fully coupled SiB-RAMS simulations.

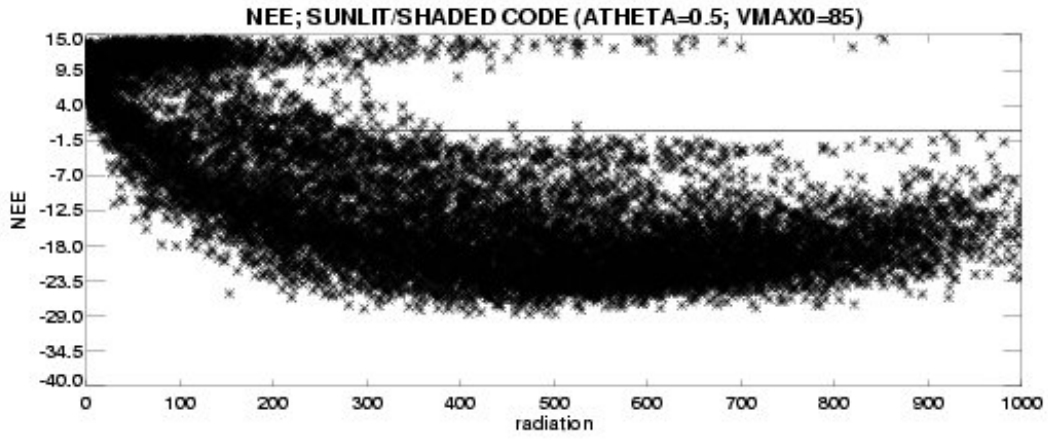

Figure 5: SiB-SUSHI NEE vs. radiation for Tapajos River km83 Tower.

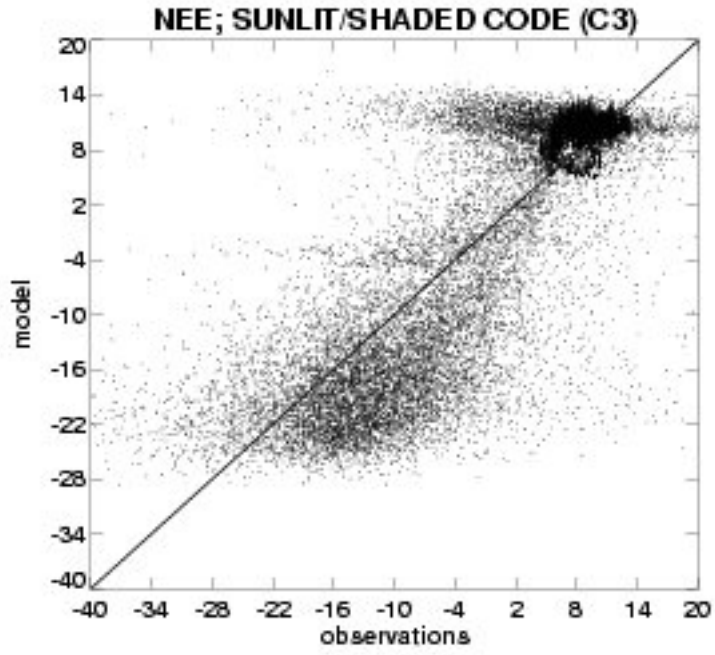

Figure 6: Observed NEE (X-axis) vs. Modeled (SiB-SUSHI) for the Tapajos River km83 Tower.

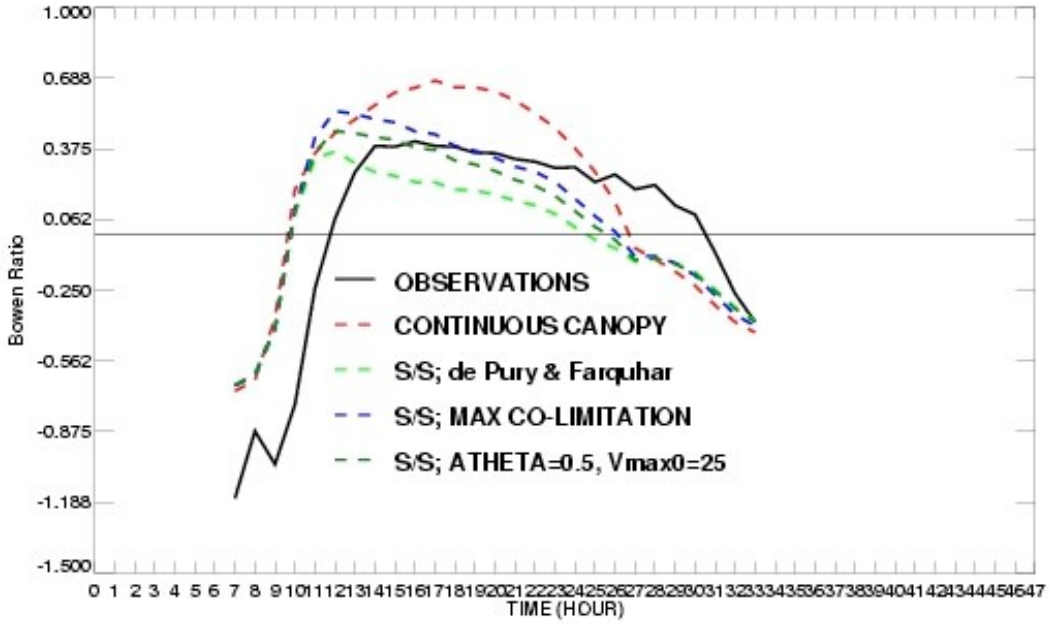

Figure 7: Bowen Ratio at Tapajos River km83 Tower. Solid line-observations; dashed red-SiB-CC; blue and green dashed-various SiB-SUSHI configurations.

1.3 Reconciling models and data of Amazõnian drought stress

Anomalous die-back of tropical vegetation in land surface models coupled to climate models is often attributed to inadequate representation of rainfall, faulty soil moisture dynamics and/or an inability to correctly represent the drought tolerance of the vegetation. The model induced die-back of tropical vegetation results in a persistent lack of atmospheric moisture, high sensible heat fluxes and larger than observed excursions of the global carbon cycle in coupled simulations. To better reconcile actual observed responses of tropical vegetation to drought stress with modeled responses we have worked to improve the soil moisture and soil water stress parameterization in SiB3. In addition we have found that additional improvements were necessary to correctly characterize the response of the carbon cycle in seasonally dry Amazõnian rain forest.

In most land surface models, root fraction decreases exponentially with depth across all biomes such that when the upper soil layers dry out, evapotranspiration and photosynthesis shut down. In shallow rooted ecosystems or ecosystems where water is unavailable at depth, this is an adequate representation. However, in systems such as the seasonally dry Amazõnian rain forest, this representation is insufficient. Results from the KM83 flux tower site in the Tapajos National Forest, Santarem, Para show that transpiration and photosynthesis are maintained in a typical dry season, although in dry seasons without many periodic rain events, some stress is evident (da Rocha *et al*, 2004). Figure 8 shows observed and modeled Net Ecosystem Exchange (NEE), sensible (H) and latent (LE) heat flux for the standard version of SiB3, before any improvements were made. Notice that dry season H is too high and dry season LE is too low. Further, dry season NEE is characterized by a large efflux of carbon not evident in the observations due to very low uptake of carbon and increased soil respiration. All of the modeled fluxes (H, LE, NEE) show too much seasonality when compared with observations. To address this, we have developed and implemented a soil moisture availability and soil water stress parameterization and tested it against three years of observational data from the KM83 flux tower site (Miller *et al*, 2004).

The soil moisture availability parameterization is based on Plant Available Water (PAW). PAW is the amount of water in the soil available to the vegetation above the wilting point of the vegetation and below or equal to the field capacity of the soil. In the new scheme, the removal of water by the vegetation is weighted by the product of the root fraction and the PAW in each layer. If the soils are moist, water is drawn according to the root profile, however, when the top layers of the soil are dry the effect is to gain greater access to deeper water if it is available. Stress on the whole ecosystem is now parameterized as a function of PAW within the total root zone, independent of root distribution. The new formulation provides a more gradual response to stress in the model, marked by a smooth transition between non-stressed and stressed vegetation. This is unlike the earlier soil moisture stress parameterizations in SiB, where vegetation was either stressed or not stressed resulting in a more cliff-like behavior.

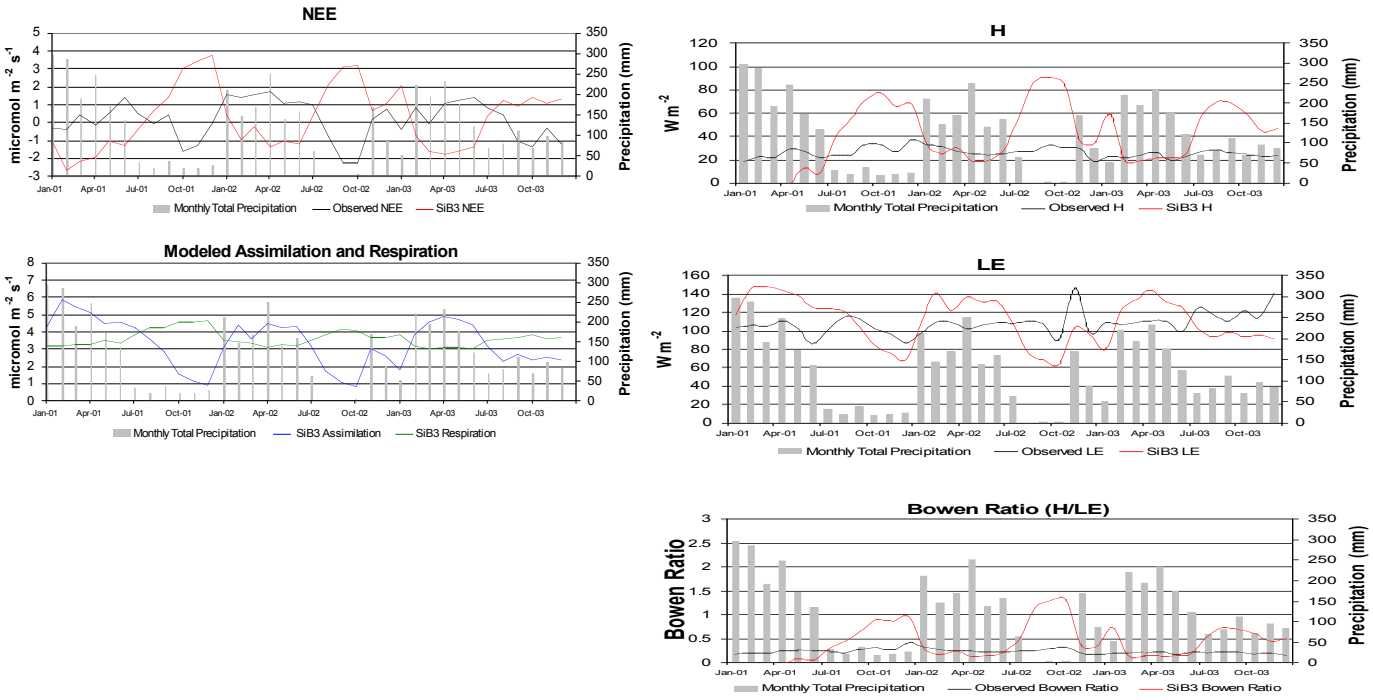

Figure 8. Monthly mean observed (black) and simulated (red) net ecosystem exchange of carbon (NEE), sensible heat flux (H), latent heat flux (LE) and bowen ratio for the standard version of the SiB3 model. Simulated assimilation (blue) and respiration (green) are also shown. During the dry seasons simulated NEE shows too much efflux because the assimilation of carbon shuts down while respiration is maintained, even increasing slightly. Simulated H is too large in the dry seasons and both simulated H and LE show too much seasonality.

However, the success of these new parameterizations in the seasonally dry Amazõnian rain forest is dependent on the availability of water at depth. Standard soil depth in SiB3 is 3.5 meters. Previous research in the Amazon has shown that larger trees are more deeply rooted than this, contributing to their access to water during the dry season (Nepstad *et al*, 1994). We have found that a combination of deeper soils and thus greater capacity for water storage and the new soil moisture availability and soil moisture stress parameterizations was necessary to improve the simulation of latent and sensible heat fluxes as well as the uptake of carbon by the vegetation. Neither the deeper soils nor the new soil water availability parameterization alone are enough to alleviate the anomalous stress in the model. Figure 9 shows observed and modeled Net Ecosystem Exchange (NEE), sensible (H) and latent (LE) heat flux for SiB3 with soil depth increased to 10m and the new soil water availability and soil moisture stress parameterizations. The increase in soil depth and available soil moisture brought the simulations much closer in line with the observations. All fluxes (H, LE, NEE) showed much less seasonality. Dry season transpiration and assimilation were maintained better, though there was still too much efflux of carbon towards the end of the dry season.

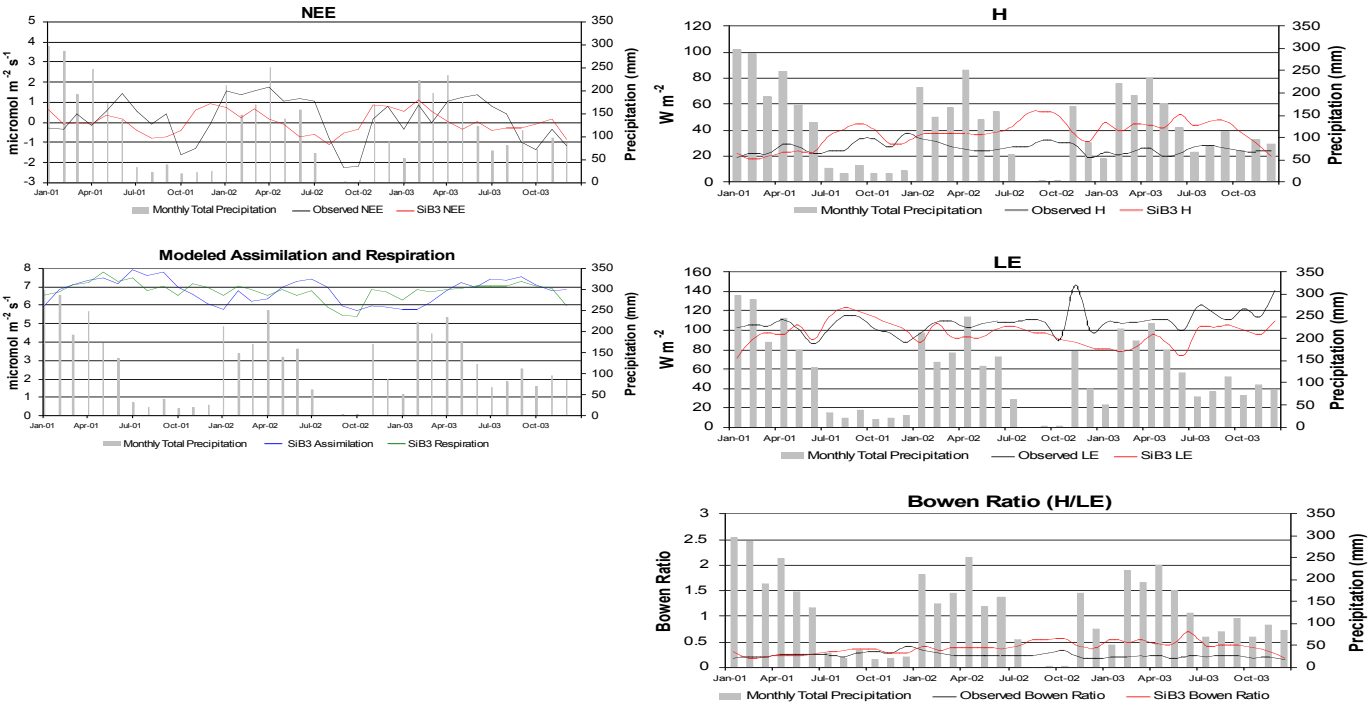

Figure 9. Monthly mean observed (black) and simulated (red) net ecosystem exchange of carbon (NEE), sensible heat flux (H), latent heat flux (LE) and bowen ratio for the version of SiB3 that includes the new soil water availability and soil moisture stress parameterization as well as deeper soils. Simulated assimilation (blue) and respiration (green) are also shown. Though simulated H is still slightly higher than observed, both simulated H and LE are much more closely in-line with the observations, this is reflected in the bowen ratio. With the new parameterizations, assimilation is now maintained during dry seasons, however there is still an offset in the seasonality of simulated NEE compared to observed NEE. There continues to be too much efflux in the simulations during the dry season.

Incorporating plant available water and deeper soil brought modeled sensible and latent heat fluxes much closer in line with observations. However, the seasonality of carbon flux was still offset. Results from the KM83 flux tower site suggest that heterotrophic respiration is very sensitive to soil moisture, with heterotrophic respiration shutting down when conditions become too dry (Goulden *et al*, 2004). The response of the heterotrophic respiration in SiB3 is dependant on both soil temperature and soil moisture. However, we found that given the great seasonality in rainfall and as well the soil characteristics in this region, the response of heterotrophic respiration to soil moisture content in SiB3 was too weak. We increased the sensitivity of the heterotrophic respiration in SiB3 to changes in soil moisture by altering the optimal soil moisture for respiration. This resulted in a much closer fit of modeled net ecosystem exchange of carbon to observations. Figure 10 shows the improved seasonality of carbon flux when this sensitivity is accounted for.

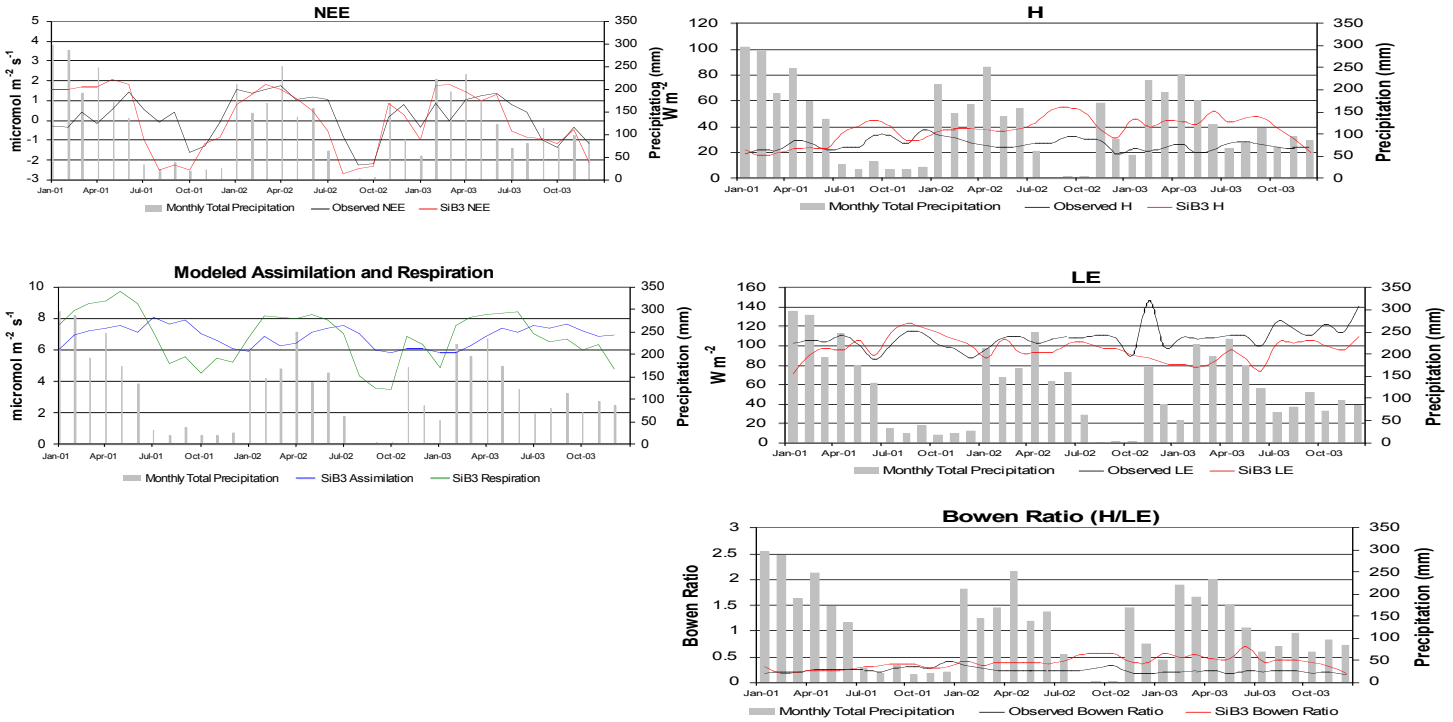

Figure 10. Monthly mean observed (black) and simulated (red) net ecosystem exchange of carbon (NEE), sensible heat flux (H), latent heat flux (LE) and bowen ratio for the version of SiB3 that includes the new soil water availability and soil moisture stress parameterization, deeper soils and increased sensitivity of heterotrophic respiration to moisture. Simulated assimilation (blue) and respiration (green) are also shown. Heterotrophic respiration now shows much more sensitivity in the dry season. Efflux of carbon is reduced while assimilation is maintained. Simulations of NEE now track observed NEE much more closely through the dry season and wet seasons as well.

Common formulations of land surface models are challenged by ecosystem dynamics in tropical forests. Improving soil moisture availability and soil moisture stress parameterizations in SiB3 improved the simulation of latent and sensible heat fluxes and net photosynthesis. However, the seasonality of carbon fluxes was not properly addressed with improvements in soil water availability alone. Improved sensitivity of heterotrophic respiration to dry season moisture stress was key to providing accurate simulations of NEE. This combination of model improvements may help to prevent the 'dry tropics' problem in coupled simulations. These results are being prepared for a publication that will focus on adjustments to soil and water stress parameterizations needed in complex land surface models for adequate simulations of the moist tropical forest biomes (Prihodko et al, in preparation).

1.4 Mesoscale circulations and atmospheric CO_2 variations in the Tapajos Region simulated by CO2RAMS

Mesoscale circulations and atmospheric CO_2 variations of Santarém area in Pará, Brazil, during the dry season 2001, were numerically investigated using CO_2RAMS with prescribed surface CO_2 fluxes according to land cover type. Four-level of nested grids drive by CPTEC analysis product were used to reproduce observed meteorology, where the finest grid is at1-km grid-spacing (Figure 11). Model evaluation against flux tower

observations and the SMC field measurements showed that, in many respects, the model is doing a reasonable job simulating the observed meteorological variables and CO_2 concentrations. The model-observation discrepancies can largely be accounted for by the fact that the model simulates conditions above the canopy whereas the observations were taken near the surface.

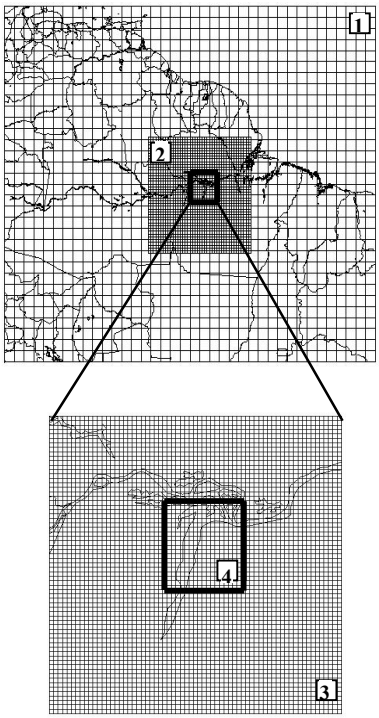

Figure 11: Nested grids used for Santarém mesoscale numerical experiments.

The mechanisms that lead to better-organized low-level cumulus clouds on the east side of the Tapajós River were explored. The most significant finding is that low-level convergence zones occur not only during weak trade wind conditions, when thermally-forced river breezes form, but are also evident on strong trade wind days. The numerical simulations illustrate that local topographic and landscape features, along with differences in roughness lengths between land and water, create a channeling effect that mechanically forces the surface winds to turn from the Amazon to the Tapajós River (Fig. 12). This subsequently leads to lower atmospheric wind to converge near the east-side of Tapajós River. Differential heating between the land and water exists and has a strong diurnal cycle. However, the resulting river breezes are not strong enough to reverse the easterlies at the surface during the dry-season strong-trade episode; it can only slow down the surface wind, and allow more upward transport of moisture from river to the cumulus clouds. The observed and simulated timings of LLC formation seem rather random. The lack of a predetermined diurnal cycle itself suggests the lesser importance of thermal forcing mechanism. The role of mechanical forcing verses thermal forcing in the formation of LLC deserves a detailed investigation in itself [*Lu et al.,* 2004]. We also performed a vorticity budget analysis, and found that solenoidal forcing associated with differential heating was not significant (figures not shown).

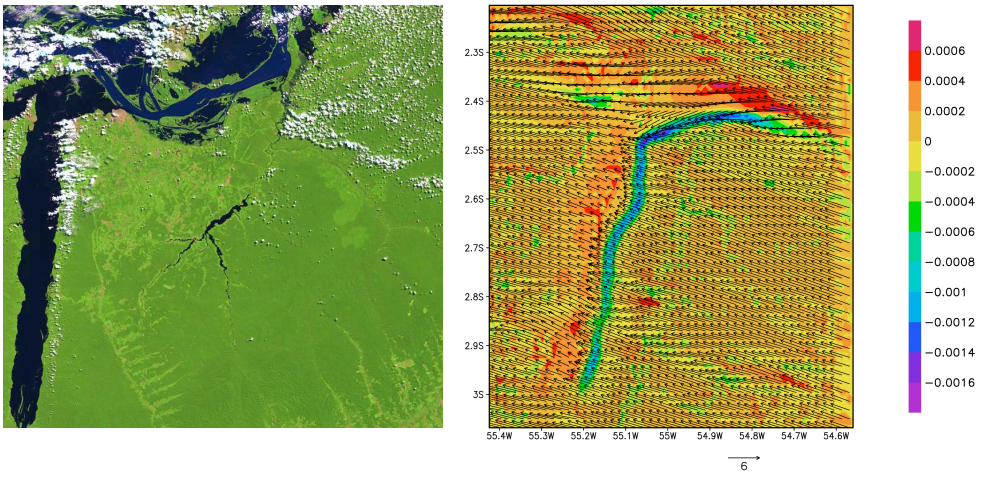

Figure 12 : A typical Landsat 7 ETM+ scene of the Tapajos region (left panel), shows that lower level cumulus clouds favor the east bank of Tapajos River. Simulated wind vectors and divergence at 57 m above ground level at noon on Aug 3, 2001 (right panel) indicate that mechanical rather than thermal forcing focuses low-level convergence in the vicinity of LBA flux towers under trade wind conditions.

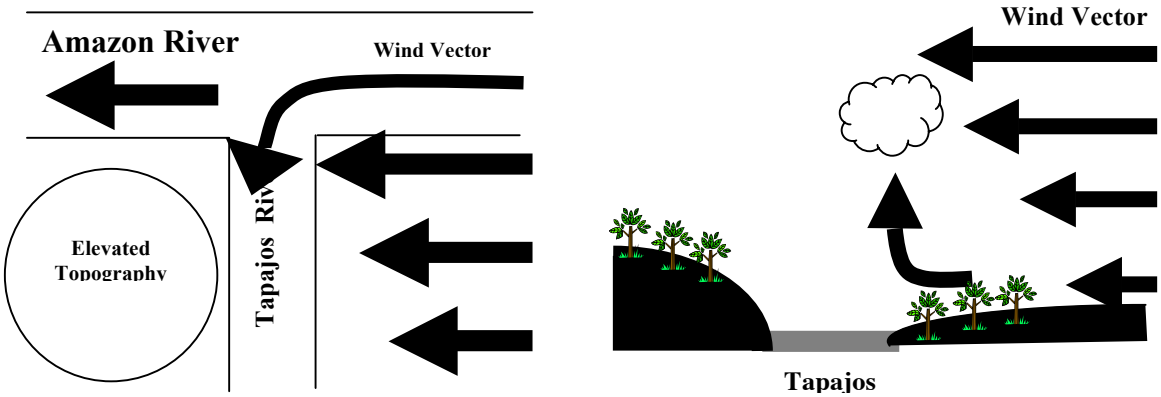

Figure 13. Conceptual diagrams showing the mechanisms that lead to the low-level convergence line on the east bank of Tapajos River, (a) horizontal distribution, (b) vertical cross section.

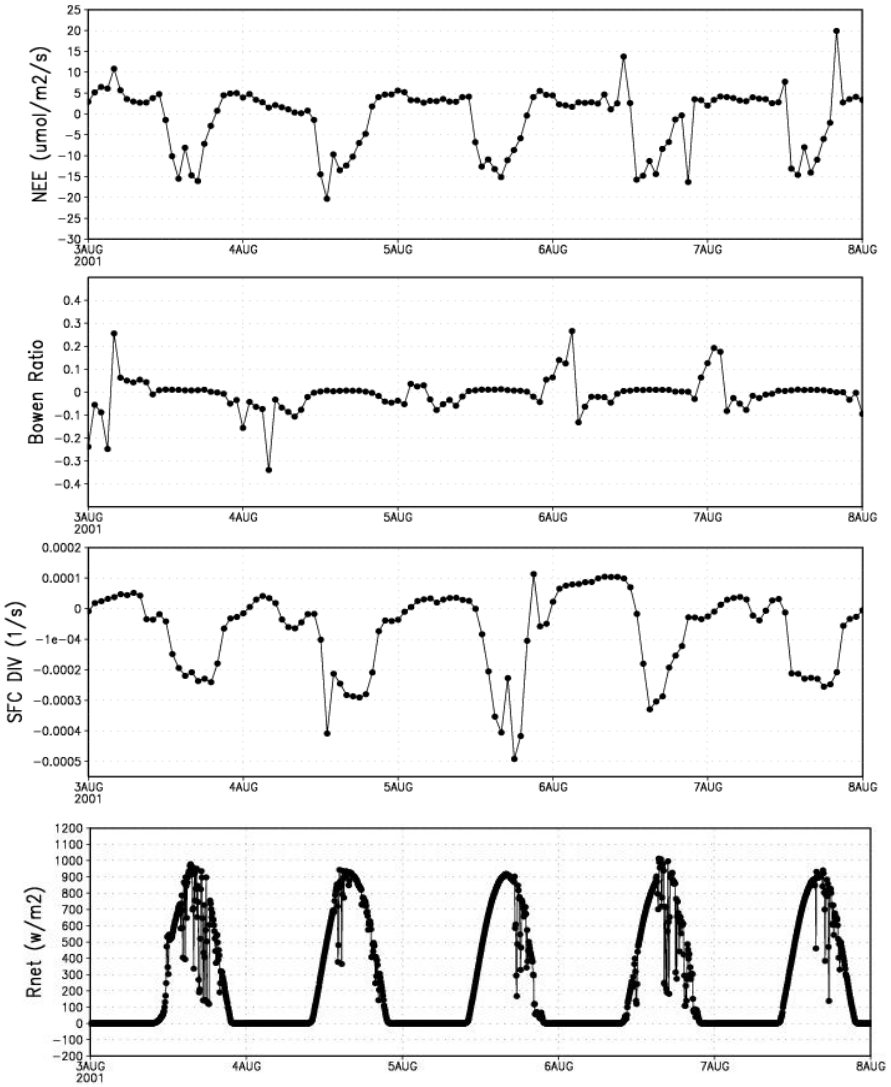

Figure 14. Observed net ecosystem exchange (NEE) and Bowen Ratio at flux tower Km 67 compared with simulated surface divergence at the same location. Also shown is the observed net radiation at Belterra meteorological tower for the same time period.

The unique physical setting of the Tapajos National Forest with respect to both the juxtaposition of the large Amazon and Tapajos Rivers may produce a unique mesoscale and micrometeorological environment. The diurnal cycle of mean vertical motion, radiation, and precipitation during the dry season along the east bank of the Tapajos River is substantially influenced by the unique geographic setting through a mechanically forced low-level convergence zone. Systematic diurnal variations in mean vertical velocity may have implications for the calculation of turbulent fluxes of heat, momentum, water, and carbon [*Baldocchi,* 2003]. The simultaneous enhancement of diffuse light, humidity, and vertical motion at mid-day probably also influences the vertical distribution of atmospheric CO_2, and must be treated correctly in regional inverse modeling efforts. It is also possible that the evolution of the forest ecosystem in the region reflects adaptation to enhanced mid-day cloudiness and/or precipitation relative to similar forests nearby. If so, the effects of mesoscale circulations and associated patterns of radiation, humidity, and precipitation should be accounted for when generalizing from flux tower data or upscaling to a larger region.

A better understanding of mesoscale circulations, advection, storage and drainage processes are important in the interpretation of eddy flux measurements. To quantify how CO_2 fluxes, the underlying vegetation, and the flux footprint vary with meteorological conditions, plant physiological and biogeochemical processes need to be included. As a next step in this research, a coupled SiB2-RAMS model, which can dynamically simulate the vegetation CO_2 flux responses to meteorological variations, such as cloudiness, and wind directions, will be employed, to show how both biological controls and meteorological factors influence regional-scale CO_2 prediction.

Most importantly, our numerical study suggests that detailed, high-resolution, mesoscale studies need to be undertaken for other long-term monitoring sites as well. Coarser resolution simulations will likely misinterpret various signals in CO_2 fluxes and concentrations at Santarem. Mesoscale numerical experiments can be a powerful tool to help determine the unique meteorological conditions associated with each tower, and to evaluate and identify the possible sources of systematic bias of tower measurements (Figure 14).

1.5 The further development of SIBRAMS model and its application to 2001 Santarem field campaign

SiB has been coupled to a mesoscale atmospheric model (Regional Atmospheric Modeling System, RAMS) for simulations of regional carbon flux and concentration over the midwestern United States (Denning et al 2003, Nicholls et al 2004). The Simple Biosphere Model (SiB) is a biophysical model that simulates the exchange of energy, mass and trace gases between the atmosphere and terrestrial biosphere (Sellers, 1986, Sellers et al 1996). Through the last three years, we have modified the SiB-RAMS coupled model by upgrading to SiB2.5 (Baker et al, 2003), which is notable in that the air within the canopy (Canopy Air Space, CAS) is prognostic with regard to temperature, moisture and CO2 concentration. The scheme for the prognostic CAS is based on Vidale and Stockli (2005), and result in more robust simulated values of state variables at the land surface as well as fluxes between the CAS and atmosphere. SiB2.5 has been shown to provide accurate fluxes of energy, mass and carbon on local scales (Baker et al 2003).

Furthermore, we have upgraded the linkage between RAMS and SiB with regard to gridded input such as vegetation and soil type, as well as for satellite-derived Normalized-Difference Vegetation Index (NDVI) data used to specify canopy phenology (Sellers et al 1996, Randall et al 1996). SiB compatibility with RAMS is now seamless to the end user with regard to grid location, configuration, and nesting.

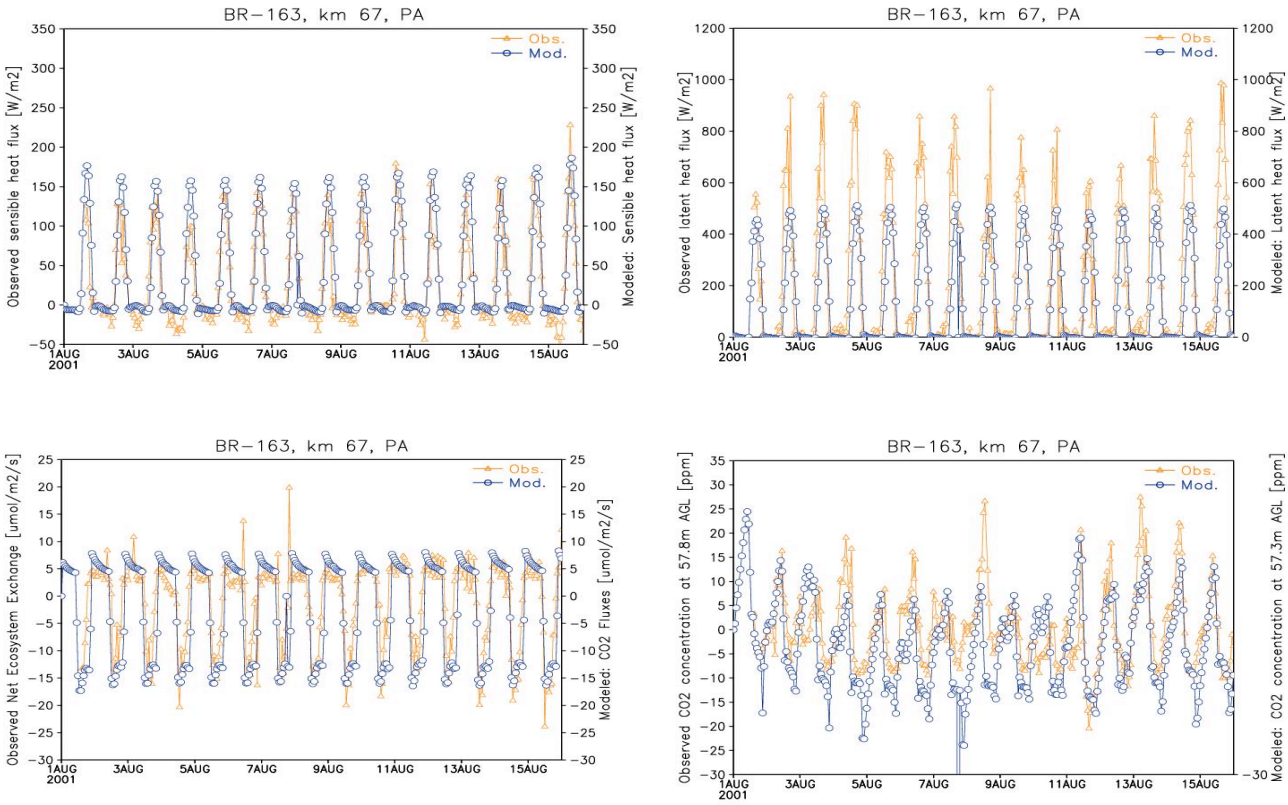

Figure 15. Observed and modeled sensible heat fluxes, latent heat fluxes, carbon fluxes (NEE), and atmospheric CO2 concentration at 57 m, for the KM 67 eddy flux tower in Santarem from August 1 through August 15, 2001.

The Simple Biosphere Model Version 2 (SiB2) is coupled with the CSU Regional Atmospheric Modeling System (RAMS) to study the two-way interactions between the land surface and atmosphere. SiB2 treats the vegetation explicitly and realistically (Baker et al. 2004), thereby incorporating the biophysical controls on the exchange of momentum, energy, water, and carbon between the two systems. The coupled SiBRAMS is used to reproduce dry season 2001 Santarem mesoscale field campaign. The simulation results are evaluated against flux tower and nearby meteorological station observations. Results from SIBRAM simulation shows good agreement between modeled and observed surface fluxes of carbon, water, and energy at the km67 flux tower site (Figure 15). At the first model level (57m), the model captures the diurnal atmospheric [CO2] variations, where the departures from average values of [CO2] are compared due to the uncertainties in [CO2] initial and boundary conditions.

Previous study using RAMS with prescribed landcover-type specific CO2 fluxes (CO2RAMS) identified a low level convergence (LLC) zone near the east bank of

Tapajos River (Lu et al. 2005). This feature is further investigated by the coupled SiBRAMS, where the feedback between the LLC and NEE is realistically captured. A comparison between SiBRAMS and CO2RAMS simulations for the same case is carried out. This highlights the impact of SiB2-calculated verses the prescribed CO2 fluxes, on simulated land-surface fluxes and near-surface meteorological conditions. We find short-term variations in CO2 flux are more accurately simulated with the more realistic canopy parameterization provided by SiB2 (Figure 14).

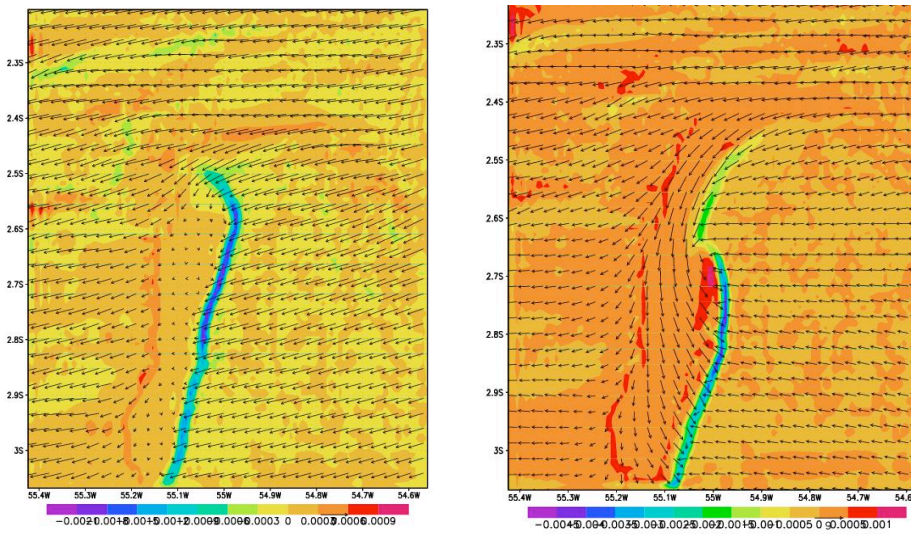

Figure 16. SiBRAMS simulated convergence line near the east bank of Tapajos River.

In addition, the mechanisms for the formation of LLC line are further explored. When the background winds turn southeasterlies, the channeling effect from the Amazon River to the Tapajos River is compromised, whereas the blocking effects of elevated topography start to take over, resulting in wind speed decreases downstream, and therefore the formation of the convergence line. Contrary to the channelling effect, in this case, the LLC line doe not form exactly along the east bank of Tapajos River; it moves in the Eastwest direction, depending on the relative strength of the background winds and the physical blocking of elevated topography. This explains why the LLC line moves eastward after sunset when winds gradually die down (Figure 16).

The persistent clouds near the east side of the Tapajos River have significant impact on observed ecosystem carbon flux and should be taken into account if tower fluxes are to be generalized to a larger region.

The role of wetlands and seasonally inundated lowlands in the Amazon Basin to regional carbon balance has also been investigated. Figure 17 illustrates spatial CO_2 concentration distribution at the lowest model level (57 m), averaged over the entire simulation time period. An increase in CO_2 concentration from the southeast to the northwest of the domain can be attributed to the steady easterly trades, the river CO_2 effluxes, and the topographic features. The maximum difference in the CO_2 concentration field is around 10 ppm between the northwest and southeast corners of the domain. At night the nocturnal land breeze (a result of differential cooling) combined with drainage flow (a result of topographic features of the river valley) creates the near-surface

horizontal transport of respired CO_2. This, in turn, promotes the accumulation of CO_2 in lowlands, leading to the higher CO_2 concentration over the Tapajos and Amazon Rivers. Prescribed river CO_2 efflux also contributes to higher overall concentrations over the entire simulation domain, but the impact is more prominent downwind, on the lee side of the rivers. Domain-averaged [CO2] shows that there is more of an impact during night than during the day, due to stable nocturnal boundary layer conditions (Figure 18).

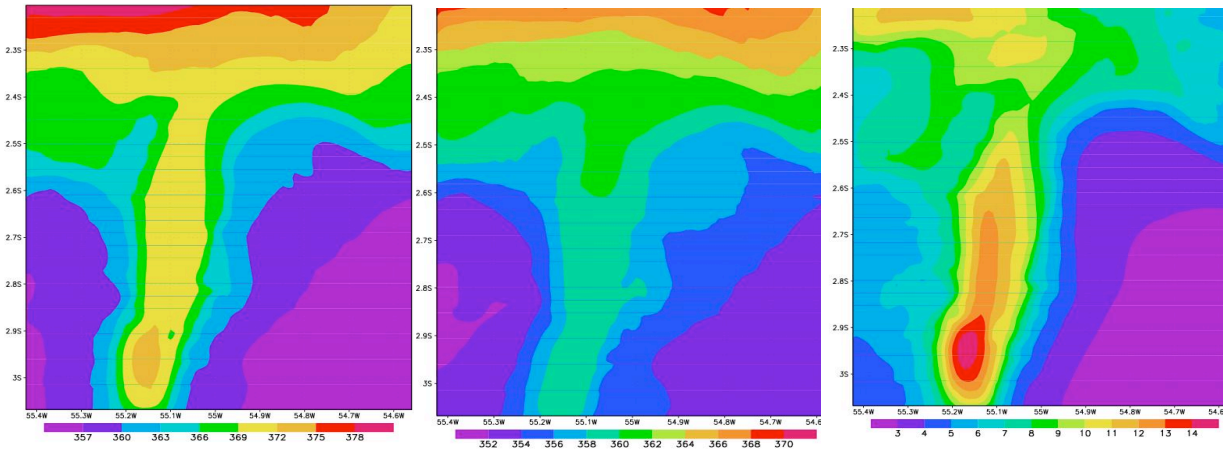

Figure 17. Spatial distribution of CO_2 concentration at 57 m, averaged from the 1st through 15th August 2001, with river co2 effluxes, without, and the difference between the first two frames.

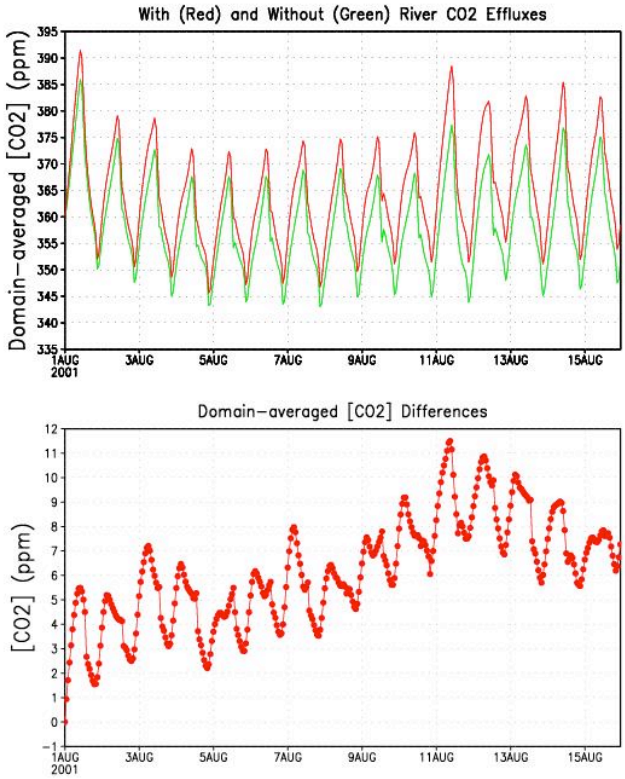

Figure 18. Domain-averaged [CO2] time series, from 1st through 15th August 2001.

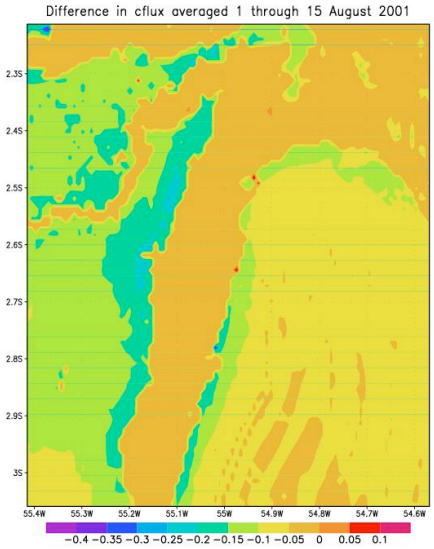

Figure 19. The difference between with the river CO2 effluxes and without in NEE averaged 1st through the 15th August 2001.

The difference in NEE between the control run and sensitivity run shows domain-wise increased CO_2 uptake over vegetated surface, due to short-term CO_2 fertilization effects. For our finest domain, 27% of the area is covered by water, and the rest is land. We assume river CO_2 effluxes are at 5 umol/m2/s based on boat measurements. Over land, the increased carbon uptake is at -0.07 umol/m2/s due to CO_2 enrichment in the atmosphere. Over both land and water, our numerical experiment shows that without river CO_2 effluxes, Amazon basin is a carbon sink, uptaking carbon at -2.12 umol/m2/s; while adding the river co2 effluxes, the basin reduces its uptake of carbon to -0.84 umol/m2/s. The CO_2 fertilization effect helps the Amazon basin stays as a carbon sink. The spatial distribution the difference in NEE due to river CO_2 effluxes shows that there is more of an impact downwind, on the lee side of the Tapajos River. However, the low-level convergence zone does bring some impact upstream against the trade, on the east side of the Tapajos River, but at a much smaller extent inland.

1.6 Evaluation of proposed sampling strategies for Balanço Atmosférico Regional de Carbono na Amazônia (BARCA) and global implications

In 2004 we participated in planning for the proposed BARCA project. BARCA will involve systematic observations of variations of trace gas mixing ratios, simulation analysis of atmospheric transport and regional flux estimation by inverse methods in an attempt to quantify regional to Basin-scale fluxes of CO_2 and test hypotheses that Amazonia is a major net source or sink for CO_2. We have conducted a series of simulation experiments that suggest that in addition to the proposed aircraft campaign for BARCA, a longer-term program of ongoing trace gas measurements may provide valuable information about the time mean carbon budget in Amazonia.

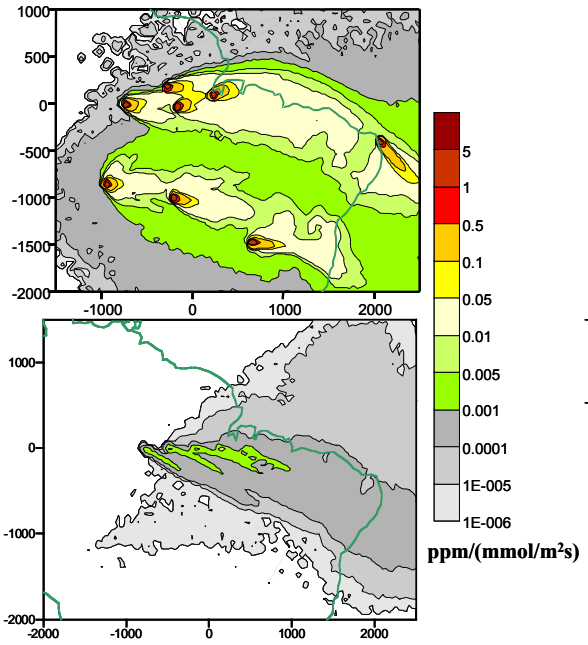

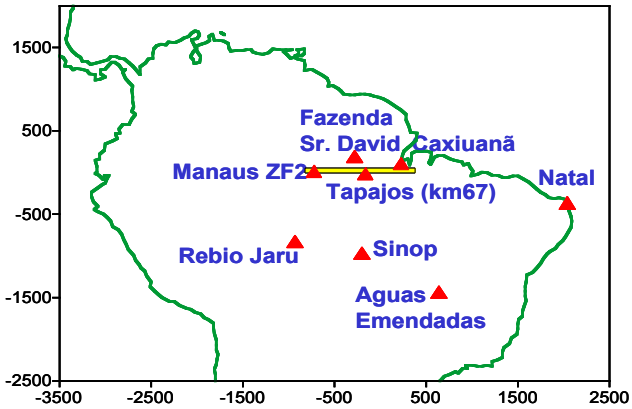

Figure 5 (above). Potential continuous CO_2 monitoring locations in Amazônia.

Figure 6 (left). Influence functions Dx Dy for (top) 50m tower sampling scheme and (bottom) a single aircraft flight

To test the different sampling schemes, aircraft vs. longer-term tower measurements, we used a Lagrangian Particle Dispersion model driven by meteorology simulated with SiB-BRAMS for the time period July 25-August 31, 2001, coincident with the Santarem Mesoscale Campaign. In Lagrangian particle dispersion modeling, massless particles are released into simulated atmospheric winds, convective transport and boundary layer turbulence. Some population of the particles reaches detectors, carrying information about their release points and time of origin. This results in spatial maps of the relative influence of different parts of the land surface on simulated observations made at the release points. We tested two sampling schemes, one with 8 50m towers operating continuously in August 2001, releasing particles each hour (Figure 5) and one with an aircraft simulating vertical profiles (10 samples over a 10 km depth) every hour (~300 km), from west to east for a 5 hour flight, releasing particles at each sample point. Our results suggest that continuously operating towers have the potential to provide information over a much larger proportion of the landscape than observations that must be collected over a limited amount of time during a flight (Figure 6).

We also evaluated the value of additional continuous [CO_2] observations in the Bayesian synthesis inversions of 12 different global tracer transport models, each run with TransCom protocols (Gurney et al, 2002). Monthly mean CO_2 flux estimates were produced for each of the 22 TransCom basis regions. Each model was run first using flask data collected at 77 sites in the remote marine boundary layer and second with the addition of 12 potential [CO_2] observing sites in and near the Amazon basin (Figure 7). For each model there was a dramatic improvement in the confidence of basin wide CO_2 flux estimates for the inversions with the additional Amazon observing sites. The addition of the 12 potential observing sites to the initial 77 flask locations reduced the average uncertainty of CO_2 flux estimates in the Amazon basin from 0.73 Gt C yr^{-1} to 0.17 Gt C yr^{-1}. Thus, our recommendation for BARCA of continuous tower based high precision [CO_2] measurements includes the additional benefit of reducing uncertainty in global atmospheric inversions and therefore in our understanding of the global carbon budget.

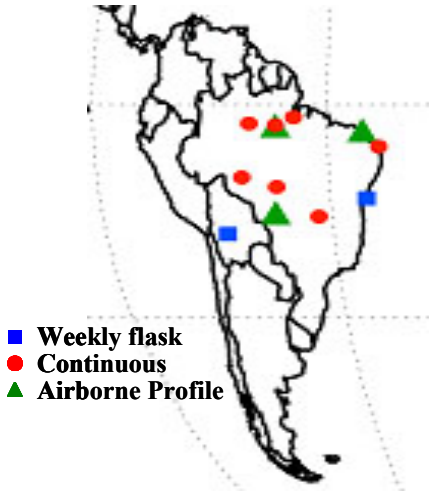

Figure 7. 12 additional [CO_2] observing sites in and around Amazônia.

1.7 Using A High-Resolution Model to Estimate Representation Errors in Inversions of Orbiting Carbon Observatory (OCO) CO_2 Retrievals

Variations of atmospheric CO_2 concentrations contain information about sources and sinks with which air interacts with as it is transported from place to place. Using atmospheric tracer transport models, inverse modelers can quantitatively estimate the strengths and spatial distribution of sources and sinks around the world from concentration data. Satellite CO_2 measurements have the potential to help inverse modeling studies by improving the data constraint due to their global spatial sampling and sheer data volume. The Orbiting Carbon Observatory (OCO), scheduled to launch in 2008, will retrieve global total column CO_2 concentrations at 1:15 PM LST with 0.5% precision. These satellite measurements can be used in inversion models to enhance our understanding of the carbon cycle; however, several errors can be introduced when using satellite measurements to optimize CO_2 concentrations in inverse studies: spatial representativeness errors may be introduced into inversions that compare CO_2 concentrations from a model grid cell to satellite concentrations sampled over only a fraction of the domain, local clear-sky errors may exist in inversions from comparing concentrations in a grid cell that may be partially cloudy to satellite mixing ratios sampled at the same time but only over clear areas, and temporal sampling errors can result from comparing OCO measurements sampled at 1:15 PM to temporally averaged concentrations in an inversion.

We investigated these errors by performing a fifteen-day simulation in August 2001 centered over the Tapajos River in the Brazilian Amazon using a coupled ecosystem-atmospheric model, SiB2-RAMS. We analyzed a fine domain of 97 by 97 km domain with 1 km horizontal resolution and a coarse domain with 5 km resolution

over a 335 by 335 km region. Using the generated CO_2 field, we compared the clear-sky total column concentrations from emulated satellite tracks to the mean total column mixing ratio over the domain. The emulated satellite tracks in our study mimicked the OCO sampling strategy: we used total column concentrations, we assumed the satellite tracked due south, we analyzed the concentrations at 1 PM, we averaged zonally adjacent pixels to create a track width of 10 km, and we meridionally averaged the concentrations to produce one emulated concentration for the entire grid cell. Using this methodology, the fine grid has 88 different possible satellite tracks at any one point in time. To analyze the results, we compiled the errors from each of the different possible tracks and from each of the different days into sampling distributions.

Both the spatial errors and the local clear-sky errors on the fine domain are considerably smaller than the instrumental error; however, the representativeness of the measurements will depend on the size and the heterogeneity of the domain the measurements are representing. The errors are smaller for the fine domain because the total-column variability at 1 PM on that scale is limited, typically <1.0 ppm. As the domain size and heterogeneity increases, the spatial variability in the domain increases. The small local clear-sky errors for both domains suggests that the errors in the total column concentration due to altered photosynthesis on cloudy vs. clear conditions are very small and that the local clear-sky errors are primarily due to advection rather than the biology. To prevent introducing spatial representation and local clear-sky errors, inverse models should use the finest resolution possible and should obtain fluxes by optimizing concentrations over regions with relatively homogeneous vegetation coverage.

The dominant source of error in the simulation was temporal sampling errors, which are errors that can be introduced into an inversion if the model uses satellite concentrations, taken only in clear conditions at 1:15 PM, to optimize temporally-averaged concentrations. The compiled distribution for the diurnal sampling errors, where the emulated satellite concentrations were compared to the domain-averaged diurnal mean, it shows a considerable range of errors for both the small and the large domain, indicating that satellite will not be able to represent a diurnal mean. In addition, we compared emulated satellite measurements to the domain-mean concentration from the entire simulation. These errors are also large and again indicate that significant errors can occur when single point measurements are used to represent temporal averages. To avoid temporal sampling errors, inverse models will have to accurately model the synoptic-scale atmospheric transport, and inversions will have to sample the modeled concentrations at the same time and location as the satellite.

References

Baker, I.T., A.S. Denning, N. Hanan, L. Prihodko, M. Uliasz, P.-L. Vidale, K. Davis and P. Bakwin, 2003: Simulated and Observed Fluxes of Sensible and Latent Heat and CO2 at the WLEF-TV Tower using SiB2.5. Global Change Biology, 9, 1262-1277.

Cassel, D.K. and D.R. Nielsen, 1986: Field Capacity and Available Waer Capacity. pp. 901-926, in: A.Klute (ed) Methods of Soil Analysis. Part I. 2nd ed. Agron Monogr. 9. ASA and SSSA, Madison WI.

da Rocha, H.R., M.L. Goulden, S.D. Miller, M.C. Menton, L.D.V.O. Pinto, H.C. De Freitas, A.M.E.S. Figueira, (2004), Seasonality of water and heat fluxes over a tropical forest in eastern Amazonia, *Ecological Applications*, *14*(4), Supplement, S22-S32.

Denning, A.S., G.J. Collatz, C. Zhang, D.A. Randall, J.A. Berry, P.J. Sellers, G.D. Colello, D.A. Dazlich, 1996: Simulations of Terrestrial Carbon Metabolism and Atmospheric CO_2 in a General Circulation Model. Part 1: Surface Carbon Fluxes. Tellus, 48B, 521-542.

Denning, A.S., M. Nicholls, L. Prihodko, I. Baker, P.-L. Vidale, K. Davis, and P. Bakwin, 2003: Simulated and Observed Variations in Atmospheric CO2 over a Wisconsin Forest. Global Change Biology, 9, 1241-1250.

De Pury, D.G.G. and G.D. Farquhar, 1997: Simple Scaling of Photosynthesis from Leaves to Canopies Without the Errors of Big-Leaf Models. Plant, cell and Environment, 20, 537-557.

Goulden, M.L., S.D. Miller, H.R. da Rocha, M.C. Menton, H.C. De Freitas, A.M.E.S. Figueira, C.A.D. De Sousa, (2004) Diel and seasonal patterns of tropical forest CO_2 exchange, *Ecological Applications*, *14*(4), Supplement, S42-S54.

Jackson, R.B. J. Canadell, J.R. Ehleringer, H.A. Mooney, O.E. Sala, E.D. Schulze, 1996: A Global Analysis of Root Distributions for Terrestrial Biomes. Oecologia, 180, 389-411.

Jipp, P.H., D.C Nepstad, D.K. Cassel, C.R. De Carvaloho, 1998: Deep Soil Moisture Storage and Transpiration in Forests and Pastures of Seasonally-Dry Amazonia. Climate Change, 39, 395-412.

Meir, P., B. Kruijt, M. Broadmeadow, E. Barbosa, O.Kull, F.Carswell, A. Nobre, and P.G. Jarvis, 2002: Acclimation of Photosynthetic Capacity to Irradiance in Tree Canopies in Relation to Leaf Nitrogen Concentration and Leaf Mass Per Unit Area. Plant, Cell and Environment, 25, 343-357.

Miller, S.D., M.L. Goulden, M.C. Menton, H.R. da Rocha, A.M.E.S. Figueira, C.A.D. De Sousa, Biometric and micrometeorological measurements of tropical forest carbon balance, *Ecological Applications*, *14*(4), Supplement, S114-S126.

Nepstad, D.C. *et al*, (1994), The role of deep roots in the hydrological and carbon cycle of Amazonian forests and pastures, *Nature*, *372*, 15 December, 666-669.

Nicholls, M.E., A.S. Denning, L. Prihodko, P.-L. Vidale, I. Baker, K. Davis and P. Bakwin, 2004: A Multiple-Scale simulation of Variations in Atmospheric Carbon Dioxide using a Coupled Biosphere-Atmospheric Model. Journal of Geophysical Research, 109, D18117, doi:10.1029/2003JD004482.

Randall, D.A., D.A. Dazlich, C. Zhang, A.S. Denning, P.J. Sellers, C.J. Tucker, L. Bounoua, J.A. Berry, G.J. Collatz, C.B. Field, S.O. Los, C.O. Justice and I. Fung, 1996: A Revised Land Surface Parameterization (SiB2) for Atmospheric GCMs. Part III: The Greening of the Colorado State University General Circulation Model. Journal of Climate, 9(4), 738-738-763.

Saleska, S.R., P. Mahadevan, A. Juete, F. Cardoso, H. da Rocha, K. Didan, D. Fitzjarrald, M. Goulden, B.Krujit, A. Manzi, S. Miller, A. Nobre, C. Randow, R. Sakal, and J. Tota, 2005: Effecs of Land Use and Climate Seasonality on Carbon Fluxes in the Amazon: Scaling from Landscape to Region using Data from MODIS Satellites and from a Network of Flux Towers. Abstract #B54B-04, American Geophysical Union Fall Meeting, San Francisco CA, 2005.

Sellers, P.J., , Y. Mintz, Y.C. Sud, A. Dalcher, 1986: A Simple Biosphere Model (SiB) for use within General Circulation Models. Journal of the Atmospheric Sciences, 43(6), 505-531.

Sellers, P.J., D.A. Randall, G.J. Collatz, J.A. Berry, C.B. Field, D.A. Dazlich, C. Zhang, G.D. Collelo and L. Bounoua, 1996: A Revised Land Surface Parameterization (SiB2) for Atmospheric GCMs. Part I: Model Formulation. Journal of Climate, 9(4), 676-705.

Sellers, P.J. S.O. Los, C.J. Tucker, C.O. Justice, D.A. Dazlich, G.J. Collatz and D.A. Randall, 1996: A Revi Revised Land Surface Parameterization (SiB2) for Atmospheric GCMs. Part II: The Generation of Global Fields of Terrestrial Biophysical Parameters from Satellite Data. Journal of Climate, 9(4), 706-737.

Vidale, P.-L. and Stockli R., 2005: Prognostic Canopy Air Space Solution for Land Surface Exchanges. Theoretical and Applied Climatology, 80(2-4), 245-257.

Wang, Y.P. and P.G. Jarvis, 1993: Influence of Shoot Structure on the Photosynthesis of Sitka Spruce (Picea Sitchensis). Functional Ecology, 7, 433-451.

2. Description of any difficulties encountered or any issues to resolve:

3. Participants:

Name: Dieter Volkhard Anhuf
Email: anhuf@usp.br
Citizenship: GERMANY

Name: Ian Baker
Email: baker@atmos.colostate.edu
Citizenship: USA

Name: Sheri Conner Gausepohl
Email: sheri@atmos.colostate.edu
Citizenship: USA

Name: Allan Scott Denning
Email: denning@atmos.colostate.edu
Citizenship: USA

Name: Maria Assuncao Faus Silva Dias
Email: assuncao@cptec.inpe.br
Citizenship: BRAZIL

Name: Rodrigo Gevaerd
Email: rodrigo@master.iag.usp.br
Citizenship: BRAZIL

Name: Kathy Corbin
Email: kdcorbin@atmos.colostate.edu
Citizenship: USA

Name: Marcos Longo
Email: marcos@master.iag.usp.br
Citizenship: BRAZIL

Name: Lixin Lu
Email: lixin@atmos.colostate.edu
Citizenship: CHINA

Name: Demerval Soares Moreira Soares Moreira
Email: demerval@master.iag.usp.br
Citizenship: BRAZIL

Name: Pedro Leite Silva Dias
Email: pldsdias@master.iag.usp.br
Citizenship: BRAZIL

Name: Lara Prihodko
Email: lara@atmos.colostate.edu
Citizenship: USA

Name: Connie Uliasz
Email: connie@atmos.colostate.edu
Citizenship: USA

Name: Marek Uliasz
Email: marek@atmos.colostate.edu
Citizenship: POLAND

4. Description of training activities conducted, including lectures, public outreach, and short courses:

Upper air measurements with balloons; radiosonde receiving station installed to track sondes that are launched in balloons every three hours.

5. Data set descriptions, including status of metadata registration and online data availability

Data Set Title: Coupled Simulations of Physical Climate and CO2 Exchange in Rondonia

Data Set Title: Simulations of Physical Climate and CO2 Exchange in Rondonia and Para

http://lba.cptec.inpe.br/poster/CD-01/Elicia_Belem_jun00.ppt

http://lba.cptec.inpe.br/posters/CD-01/Denning/lixin.agu2001.ppt

http://lba.cptec.inpe.br/posters/CD-01/Denning/cmdl.ppt

http://lba.cptec.inpe.br/posters/CD-01/Denning/AtlantaIsotopes.ppt

http://lba.cptec.inpe.br/posters/CD-01/Denning/LBA.Belem.poster.ppt

http://lba.cptec.inpe.br/posters/CD-01/Denning/AtlantaInversions.ppt

http://lba.cptec.inpe.br/posters/CD-01/Denning/aguwide.ppt

http://lba.cptec.inpe.br/posters/CD-01/Denning/Elicia_AGU_dec00.ppt

ftp://lba.cptec.inpe.br/lba_archives/CD/CD-01/Inazawa/1108.dat
label: data collected on Aug 11th

ftp://lba.cptec.inpe.br/lba_archives/CD/CD-01/Inazawa/1308.dat
label: data collected on Aug 13th

ftp://lba.cptec.inpe.br/lba_archives/CD/CD-01/Inazawa/1408.dat
label: data collected on Aug 14th

ftp://lba.cptec.inpe.br/lba_archives/CD/CD-01/Inazawa/1508_11h.dat
label: data collected on Aug 15th - 11am

ftp://lba.cptec.inpe.br/lba_archives/CD/CD-01/Inazawa/1508_16h.dat
label: data collected on Aug 15th - 4pm

6. List of publications

Journal Publications

Baker, I.T., A.S. Denning, G.J. Collatz, J.A. Berry, L. Prihodko, N. Hanan, K.M. Schaefer, A.W. Philpott, N. Suits, O. Leonard, 2006: The Next Generation Simple Biosphere Model (SiB3). Part I: Model Formulation. In preparation.

Silva Dias, M. A. F., P. L. Silva Dias, M. Longo, D. R. Fitzjarrald, and A. S. Denning, 2005. River breeze circulation in eastern Amazon: observations and modeling results *Theoretical and Applied Climatology, 78(103), 111-121.*

Corbin, K., A.S. Denning, L. Lu, J.W. Wang, I. Baker, 2005: Evaluating Spatial, Clear-Sky, and Temporal Errors in Inversions of Orbiting Carbon Observatory (OCO) CO2 Retrievals. In preparation.

Lu, L., A. S. Denning, M. A. da Silva Dias, P. Silva Dias, M. Longo, S. R. Freitas, and S. Saatchi (2005), Mesoscale circulation and atmospheric CO2 variation in the Tapojos Region, Para, Brazil, *J. Geophys. Res., 110,* D21102, doi: 10.1029/2004JD005757.

Lu, L., A.S. Denning, M. A. da Silva Dias, and P. Silva Dias, 2005: The potential influence of surface water CO2 effluxes on regional carbon balance in the Tapajos region, Para, Brazil. Submitted.

Lu, L., A.S. Denning, I. Baker, M.A. Silva Dias, P. Silva Dias, 2006: Simulating the two-way interactions between vegetation biophysical processes and mesoscale circulations during 2001 Santarem field campaign. In preparation.

Prihodko, L., Denning, A.S., Baker, I., *Reconciling models and data of Amazõnian Drought Stress*, in preparation.

Conference papers

Baker, I.T., 2005: Radiation Schemes in Biophysical Models: Big Leaf vs. 2-Leaf Submodel in the Simple Biosphere Model (SiB). ChEAS Annual Meeting, Kemp Research Station, WI, 01 June 2005.

Baker, I.T. 2005: 2-Leaf Radiative Submodel Coupled to a Fully Prognostic Canopy Airspace Land Model (SiB3.0). CCSM Annual Workshop, Breckenridge CO, 22 June 2005.

Baker, I.T. 2005: Simple Biosphere Model in a Nutshell: Evolution, Model Scheme and Diagnostics. University of Iowa (invited), 12 July 2005.

Baker, I.T., K.M. Schaefer, A.W. Philpott, S.L. Connor Gausepohl, 2005: Effect of Phenology and Respiration Parameterization on Modeled Carbon Flux. 7th International Carbon Dioxide Conference, Boulder CO, 15 October 2005.

Baker, I.T., G.J. Collatz, L. Prihodko, K.M.Schaefer, J. Berry, A.S. Denning, 2005: Leaf-to-Canopy Scaling of Carbon, Energy and Moisture Fluxes in the Simple Biosphere Model (SiB). Abstract B51C-0228, American Geophysical Union Fall Meeting, San

Francisco CA, 09 December 2005.

Corbin, K., A.S. Denning, L. Lu, J.W. Wang, I. Baker, 2005: Evaluating Spatial, Clear-Sky, and Temporal Errors in Inversions of Orbiting Carbon Observatory (OCO) CO2 Retrievals. 7th International Carbon Dioxide Conference, 15 October, Broomfield, CO.

Corbin, K., A.S. Denning, L. Lu, J.W. Wang, I. Baker, 2005: Evaluating Spatial, Clear-Sky, and Temporal Errors in Inversions of Orbiting Carbon Observatory (OCO) CO2 Retrievals. TransCom Meeting, June 2005, Paris, France.

Corbin, K., A.S. Denning, L. Lu, J.W. Wang, I. Baker, 2005: Evaluating Spatial, Clear-Sky, and Temporal Errors in Inversions of Orbiting Carbon Observatory (OCO) CO2 Retrievals. ESA-ESRIN Carbon from Space meeting, June 2005, Frascati, Italy.

Lu, L., A.S. Denning, M.A. da Silva Dias, P. Silva-Dias, M. Longo, S.R. Freitas, and S. Saatchi, 2005: Mesoscale circulation and atmospheric CO2 variation in the Tapajos Region, Para, Brazil. AMS annual meeting, January 10-14, 2005, San Diego, CA.

Lu, L**.**, A.S. Denning, and I. Baker, A. Wang, and K.D. Corbin, 2005: Simulating the two-way interactions between vegetation biophysical processes and mesoscale circulations during 2001 Santarem field campaign. The Seventh International Carbon Dioxide Conference (ICDC7). September 25-30, 2005, Boulder, CO.

Prihodko, L., Denning, A.S., Baker, I., 2005, Modeling Drought Tolerance in Amazõnia with Sib3**,** Community Climate System Model Annual Workshop, June 21-23, Breckenridge. CO, USA

Prihodko, L., Denning, A.S., Baker, I., 2005, Modeling Drought Tolerance in Amazõnia with Sib3, International Postdoctoral Scientist Network for Earth System Science, June 23-25, Breckenridge. CO, USA

Prihodko, L., Denning, A.S., Baker, I., 2005, Modeling Drought Tolerance in Amazõnia with Sib3, International Carbon Dioxide Conference 7, September 25-30, Broomfield. CO, USA.